

Journal of Materials Chemistry A

Accepted Manuscript



This is an *Accepted Manuscript*, which has been through the Royal Society of Chemistry peer review process and has been accepted for publication.

Accepted Manuscripts are published online shortly after acceptance, before technical editing, formatting and proof reading. Using this free service, authors can make their results available to the community, in citable form, before we publish the edited article. We will replace this *Accepted Manuscript* with the edited and formatted *Advance Article* as soon as it is available.

You can find more information about *Accepted Manuscripts* in the [Information for Authors](#).

Please note that technical editing may introduce minor changes to the text and/or graphics, which may alter content. The journal's standard [Terms & Conditions](#) and the [Ethical guidelines](#) still apply. In no event shall the Royal Society of Chemistry be held responsible for any errors or omissions in this *Accepted Manuscript* or any consequences arising from the use of any information it contains.

Ammonium-based Protic Ionic Liquid Doped Nafion Membrane as Anhydrous Fuel Cell Electrolyte[†]

Anurag Prakash Sunda^{*a,b}

Received Xth XXXXXXXXXXXX 20XX, Accepted Xth XXXXXXXXXXXX 20XX

First published on the web Xth XXXXXXXXXXXX 200X

DOI: 10.1039/b000000x

Polymer Electrolyte Membrane doped with Protic Ionic Liquids (PILs) can serve as promising materials for anhydrous proton conduction. In the present study, Molecular Dynamics simulations are performed to characterize the structure and dynamics of diethylmethylammonium triflate ([dema][TfO]) PIL doped Nafion membrane at various PIL doping and temperature. The polymer membrane PIL interface structure shows that the hydrogen bonding interactions predominantly exist between the acidic site (N–H) of the ammonium cation and SO₃[−] group of [TfO[−]] anion or Nafion. The distribution of SO₃[−] group (of [TfO[−]] anion or Nafion) around the ammonium cation increases with PIL concentration. The existence of weak hydrogen bonding interactions between the alkyl hydrogen atoms of the [dema⁺] and the SO₃[−] group of Nafion remain unaffected by PIL concentration. An increase in PIL doping level and temperature results in faster diffusion (higher ionic conductivity) which is in qualitative agreement with experiments.

Keywords: Fuel Cells, Polymer Electrolyte Membrane, Protic Ionic Liquids, Molecular Dynamics, Ionic Conductivity.

1 Introduction

The use of ionic liquids (ILs) as hybrid electrolytes or dopant have spurred immense interest for their potential use in emerging energy technologies.^{1–11} A remarkable enhancement in thermal, mechanical, and electrochemical properties of ionic liquid based composite membranes have advanced the development of anhydrous membrane electrolytes.^{12–23} Nakamoto and Watanabe²⁴ observed superior electrochemical properties for N,N-diethyl-N-methylammonium triflate ([dema][TfO]) protic ionic liquid (PIL) under anhydrous condition. Watanabe and co-workers^{12,17} examined thermal and electrochemical properties of [dema][TfO] PIL doped composite membranes and obtained high ionic conductivity under anhydrous conditions. The authors also achieved considerable improvement in activity of H₂/O₂ reactions at the platinum electrode.

The role of cation-ionomer interactions in polymer-PIL composite is crucial and has significant influence on ionomer

nanostructure and interionic charge transfer. The characterization of nanostructure and dynamical properties of IL doped composite membranes by Iojoiu and co-workers^{13–16,18,21} showed that the existence of ionic clusters in membrane matrix leads to a pronounced effect on charge transfer. Zheng and co-workers^{19,20} explored thermal, mechanical and dynamic properties of Nafion membrane doped with various PILs. Apart from improved thermal stability and conductivity, the authors observed that PILs with longer alkyl tail length shows phase separation with the membrane.

The interionic interactions in ammonium based ILs are critical for the electrochemical properties of electrolytes. Platinum electrode kinetics with [dema][TfO] studied by Johnson et al.²⁵ at varying temperature for H₂ and O₂ gases showed improved electrode kinetics at higher temperature (>100 °C). Molecular Dynamics (MD) simulation study of Sunda et al.²⁶ on benzyltrialkylammonium trifluoromethanesulfonate ILs have shown that the presence of C–H/phenyl interactions have a pronounced effect on ionic conductivity. Subsequently, Sunda et al.²⁷ examined the influence of steric effects on dynamics of ammonium triflate PILs by varying alkyl groups (methyl, ethyl, and *n*-propyl) on the ammonium cation. The authors concluded that an increase in the alkyl tail length leads to a decrease in electrical conductivity. The influence of adsorbed ions of room temperature ILs on ionic liquid-platinum electrode interface was studied by Ejigu and Walsh²⁸ using [dema][TfO], and [dema] bis-(trifluoromethanesulfonyl)imide ([dema][Tf₂N]) ILs. The authors found an anion selective ad-

[†] Electronic Supplementary Information (ESI) available: [Simulated annealing temperature as a function of simulation time is shown in Figure S1. RDFs for PIL interactions at 393 K are shown in Figure S2 and Figure S3. Structure factor and scattering intensity at 393 K is shown in Figure S4 and Figure S5 respectively. For all Nafion:PIL ratio, the β plot for cations and anions is shown in Figure S6.] See DOI: 10.1039/b000000x/

^aChemistry and Physics of Materials Unit, Jawaharlal Nehru Centre for Advanced Scientific Research, Bangalore 560064, INDIA.

^bMaterials Research Laboratory, Department of Chemistry, Pandit Deendayal Upadhyay Shekhawati University, Sikar 332001, Rajasthan, INDIA. Fax: +91 (1572) 273100; Tel: +91 (1572) 273200; E-mail: anurag.sunda@gmail.com, anurag@jncasr.ac.in

Table 1 Total number of atoms (N_{atoms}), box length (in Å), and density (ρ in g cm^{-3}) of [dema][TfO] doped Nafion from NPT simulations.

No. of ion pairs	N_{atoms}	Box length		Density	
		300 K	393 K	300 K	393 K
$C_{1/1}=240$	27888	70.89	71.71	1.67	1.62
$C_{1/2}=480$	34608	75.23	76.63	1.63	1.55
$C_{1/3}=720$	41328	79.39	80.91	1.58	1.50

$C_{1/1}$, $C_{1/2}$ and $C_{1/3}$ represents 1:1, 1:2, and 1:3 Nafion:PIL ratios respectively.

sorption towards the $[\text{Tf}_2\text{N}^-]$ at the platinum electrode and observed slower O_2 reduction with $[\text{Tf}_2\text{N}^-]$ compared to $[\text{TfO}^-]$ anion based PIL.

An advancement in the development of composite membranes for high temperature fuel cell application is of great interest and atomistic simulations can play vital role in characterization of such PIL doped polymer composite. Among the several PILs based on Brønsted acid-base combination of various oxoacids with aliphatic amines, [dema][TfO] was found to be a better choice for electrochemical applications compared to other PILs.²⁴ In the present work, MD simulations are employed to characterize structure and dynamics of Nafion membrane doped with varying [dema][TfO] PIL concentration at 300 K and 393 K. The proton decoupled transport phenomenon was not detected using PFG stimulated echo NMR spectroscopy study of ammonium triflate PILs^{23,29}. Hence, classical MD simulations can be used to examine the mobility of ions (vehicular mechanism) in PIL doped Nafion composite membranes. The computational details are presented in section 2. Results and discussion presented in section 3 are as follows: we examine the various interionic interactions such as hydrogen bond interactions between ammonium cation and SO_3^- group of $[\text{TfO}^-]$ anion and Nafion. The structure factor, scattering intensities, and dynamical properties (self-diffusion coefficients and Nernst-Einstein conductivity) of PIL doped Nafion membrane at varying PIL ratios and temperature are also explored. A summary of key findings concludes this paper.

2 Computational details

The chemical structures of Nafion polymer electrolyte membrane and [dema][TfO] PIL are shown in **Figure 1**. Classical MD simulations were carried out using GROMACS 4.5.4³⁰ program. Force field parameters for Nafion were taken from earlier studies.^{31,32} The [dema][TfO] PIL was modelled using force field parameters of Chang et al.³³ An energy minimized Nafion polymer chain (682 atoms) was replicated to generate 24 polymer chains. In order to make the system neutral, 240

[dema⁺] ions were added. A simulated annealing (one cycle) was performed to avoid local minima and more details of simulated annealing are shown in **Figure S1** of Supporting Information. Further, the system was solvated by 720 [dema][TfO] ion pairs. The packmol³⁴ software package was used to get initial configuration of neat [dema][TfO] ion pairs to solvate polymer chains. The simulated annealing procedure was repeated on [dema][TfO] solvated polymer chains for six cycles. Three ratios of Nafion and PIL 1:1, 1:2, and 1:3 are chosen for investigation in this study (henceforth, the PIL doped Nafion composite are called as $C_{1/1}$, $C_{1/2}$, and $C_{1/3}$). In each system, the Nafion:PIL ratio is defined as a number of [dema][TfO] ion pairs per sulfonate (SO_3^-) group of the Nafion membrane. The $C_{1/3}$ system was used as template to generate $C_{1/1}$ and $C_{1/2}$. A pre-equilibration of 5 ns using the NPT ensemble was carried out on above system configuration.

Particle Mesh Ewald (PME) method^{35,36} was implemented to compute the long-range electrostatic interactions with a precision of 10^{-5} . The pairwise interactions were calculated within a distance cutoff of 12 Å. The leapfrog algorithm was implemented to integrate equations of motion with a time step of 1 fs. The velocity-rescale thermostat³⁷ and a Berendsen

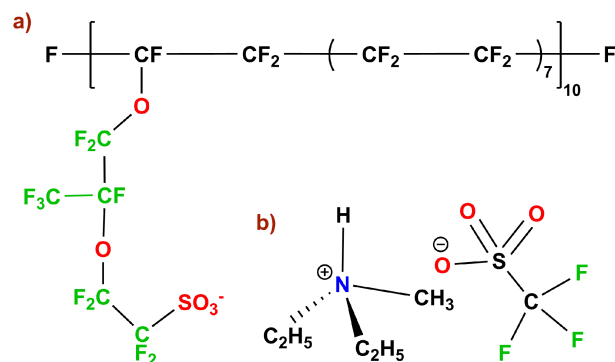


Fig. 1 The chemical structure of a) Nafion polymer electrolyte membrane and b) N,N-diethyl-N-methylammonium triflate ([N122][TfO]) protic ionic liquid.

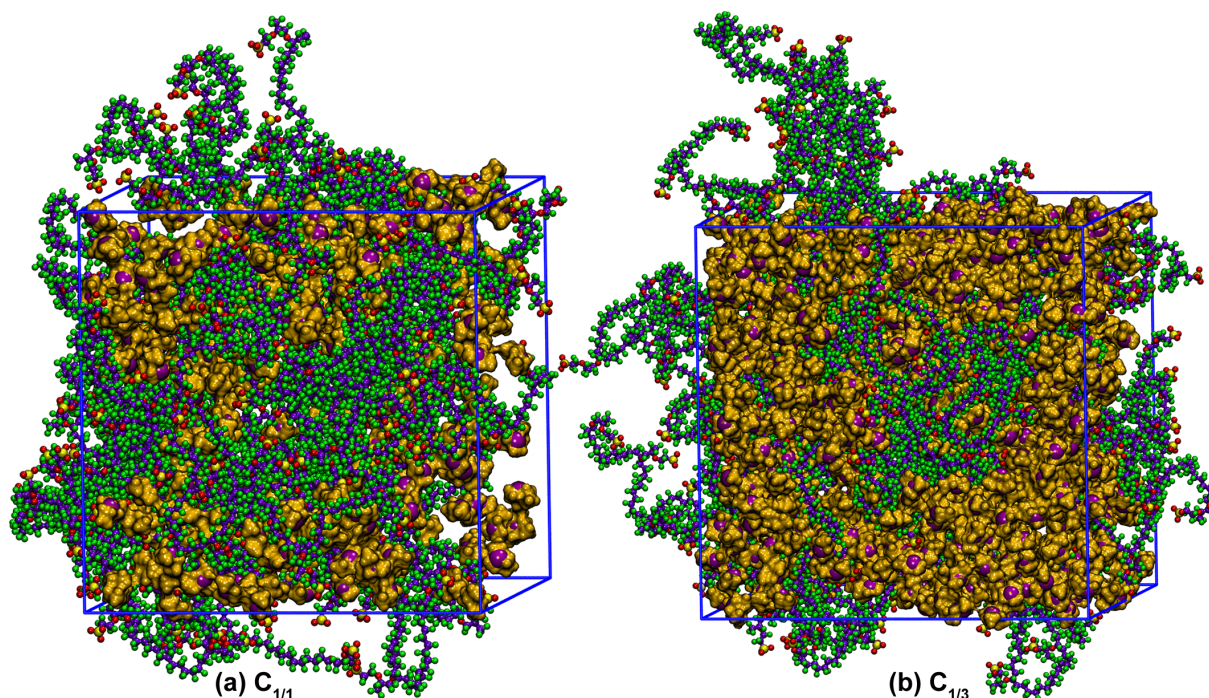


Fig. 2 Snapshots of [dema][TfO] PIL doped Nafion from production run at 393 K for a) $C_{1/1}$, and b) $C_{1/3}$. [Colour scheme for (i) [dema] cation: N–purple (CPK), C and H–orange (surface), (ii) Nafion polymer chain (CPK) C–violet, F–green, S–yellow, O–red, and (iii) [TfO] anions are not displayed for better visualization]

barostat³⁸ were employed for constant temperature and constant pressure dynamics with a coupling of 0.1 ps. MD simulations were performed at 300 K and 393 K. Pre-equilibration was extended to an equilibration of 20 ns using the NPT ensemble. Production run of 50 ns was carried out using the NVT ensemble and trajectories were recorded every 10 ps. The last 20 ns of production run was used to analyse trajectories. Visual Molecular Dynamics³⁹ was used for visual inspection of snapshots from production run and spatial density maps.

The box length and computed densities from the NPT simulations are shown in **Table 1**. Density decreases with an increase in temperature and PIL doping. The snapshots of [dema][TfO] doped Nafion from production run at 393 K are shown in **Figure 2**. As seen from the snapshots, the distribution of [dema⁺] ions is random and closer to the SO₃[−] group of Nafion. Further, self-aggregation of ions is also observed at higher PIL concentration ($C_{1/3}$) as seen in **Figure 2b**.

3 Results and Discussion

The presence of the acidic site on [dema⁺] may exhibit interionic hydrogen bonding interactions with [TfO[−]] anions and SO₃[−] group of Nafion membrane. Such hydrogen bond interactions play vital roles in determining the intermolecular

nanostructure and dynamics in PILs. We have calculated Radial Distribution Functions (RDFs), Spatial Distribution Functions (SDFs), structure factor and scattering intensities to characterize the structure of PIL doped Nafion membrane.

3.1 Radial Distribution Functions

The interfacial structural correlations of the PIL doped Nafion composite membranes are examined by the calculation of Radial Distribution Functions (RDFs)⁴⁰ from MD simulations. The RDF $g_{AB}(r)$ between the atom A and atom B can be written as:

$$g_{AB}(r) = \frac{1}{\langle \rho_B \rangle_{local}} \frac{1}{N_A} \sum_{i \in A} \sum_{j \in B} \frac{\delta(r_{ij} - r)}{4\pi r^2} \quad (1)$$

where, $\langle \rho_B \rangle_{local}$ is the atom density of atom B averaged over all the spheres and number of frames around the reference atom A . The interionic interactions characterized by RDFs are shown in **Figure 3** and **Figure 4**. In the PIL, the N-atom closely represents the center of mass of the cation and S-atom closely represents the center of mass of the anion. The cation–cation interactions of PIL from N–N RDF (see **Figure 3a**) shows a broad peak (5 to 9 Å). The peak intensity decreases with an increase in the PIL doping. **Figure 3b** shows the cation–anion interionic interactions (N–S RDF). The RDF

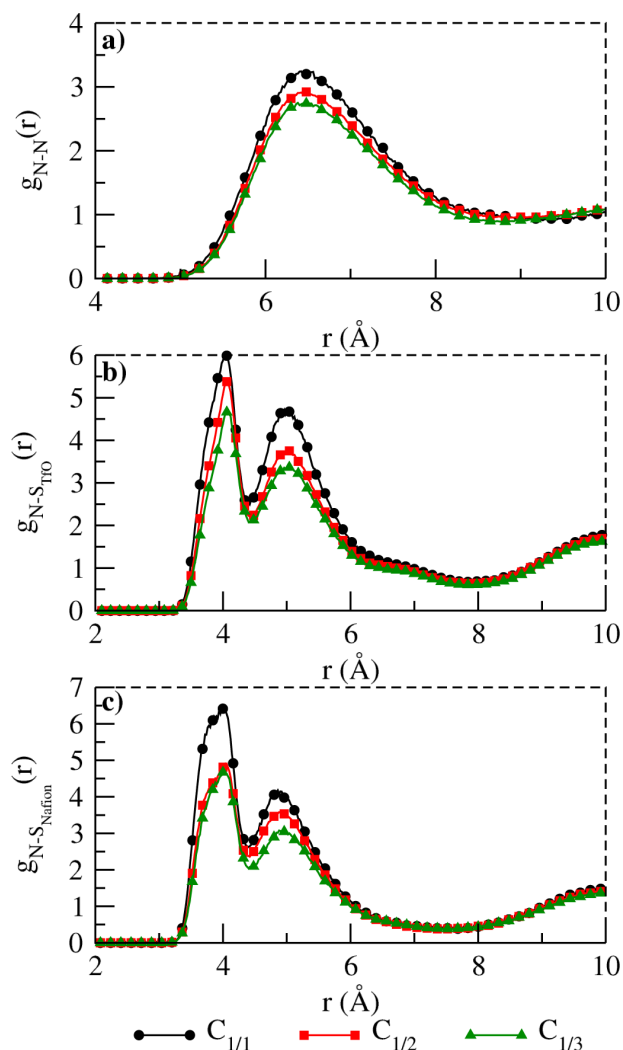


Fig. 3 RDFs calculated for ammonium cation interactions at 300 K for a) N–N, b) N–S_{TfO}, and c) N–S_{Nafion}.

profile shows a large solvation shell of 8 Å with an intense bifurcated peak at 4 Å and 5.5 Å. Similar to the cation–anion RDF, N–S RDF (see **Figure 3c**) between cation and SO₃[−] of Nafion also shows a bifurcated peak at 4 Å and 5.5 Å. The first peak in N–S RDFs (see **Figure 3b** and **c**) at ~4 Å corresponds to hydrogen bonding interactions between the acidic hydrogen attached to Nitrogen (H_N) and oxygen atoms of SO₃[−] group (of [TfO[−]] anions or Nafion) within the first solvation shell. The N–S RDF peak at ~5.5 Å arises due to the weak hydrogen bonding interactions between methyl/methylene hydrogen atoms of [dema⁺] and oxygen atoms of SO₃[−] group as shown in atomistic simulation study of Sunda et al.²⁷ on [dema][TfO] PIL. The peak intensity of N–S RDF decreases with an increase in PIL concentration. Thus, the interactions of the ammonium cations with the sulfonate groups (of [TfO[−]]

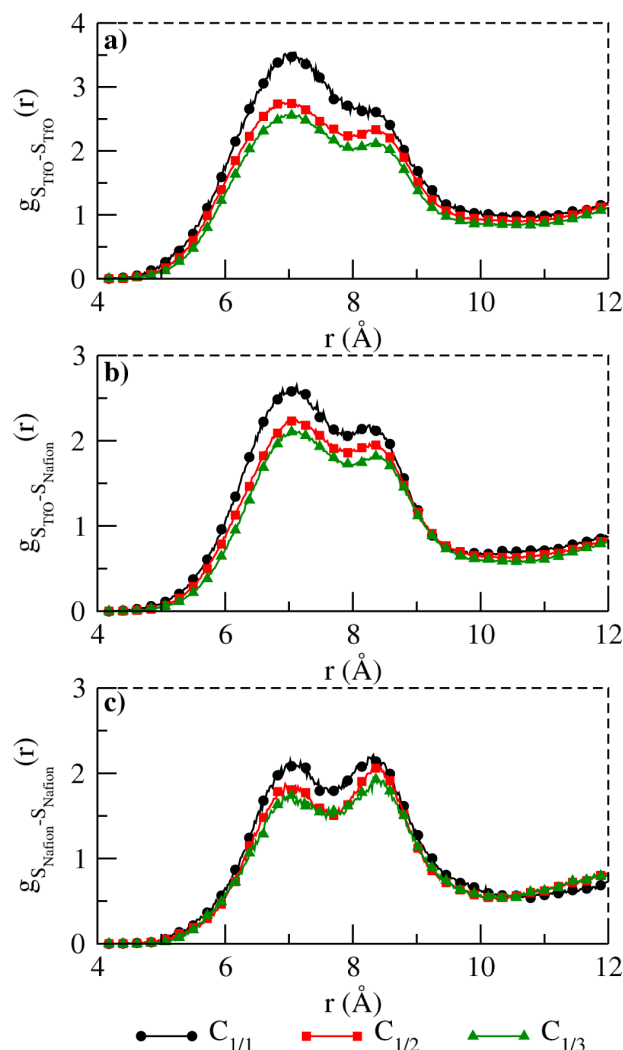


Fig. 4 RDFs calculated for sulfonate-sulfonate (S–S) interactions at 300 K for a) S_{TfO}–S_{TfO}, b) S_{TfO}–S_{Nafion}, and c) S_{Nafion}–S_{Nafion}.

anions or Nafion) decrease with PIL concentration. The effect of increases in temperature on N–N and N–S RDFs is insignificant as seen from **Figure S2** of Supporting Information.

Similar to the cation–cation RDF, the S–S RDF between the [TfO[−]] anions (see **Figure 4a**) show a broad peak (5 to 10 Å) with a head (~7 Å) and shoulder (~8.5 Å). The peak profiles in RDFs obtained for [dema][TfO] are in good agreement with those from the bulk ionic liquid simulations²⁷ on [dema][TfO]. The peak profiles seen in **Figure 4a** are found similar to the S–S RDF between the SO₃[−] group of [TfO[−]] and SO₃[−] group of the Nafion (see **Figure 4b**). The similarities in S–S RDFs peak profiles clearly suggests that [TfO[−]] anions enhance the possibility of hydrogen bond connectivity in composite membrane matrix. The S–S peak profile between the SO₃[−] groups of Nafion (see **Figure 4c**) show a good match

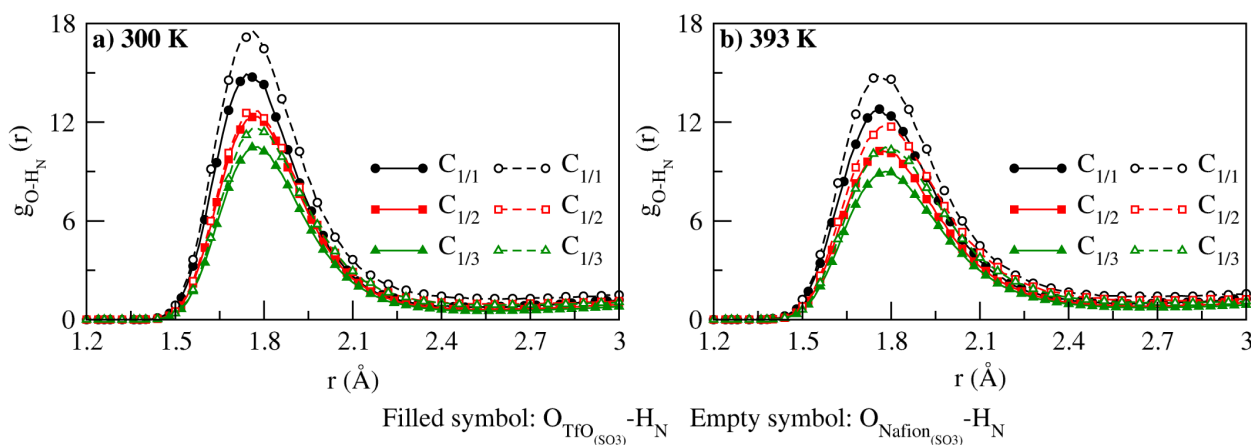


Fig. 5 RDFs for O...H hydrogen bonding interactions between oxygen atom of sulfonate group and acidic hydrogen of ammonium cation calculated at a) 300 K, and b) 393 K.

with earlier simulation studies on Nafion.^{32,41} Moreover, the structure correlations seen in S-S RDFs remains unaffected with an increase in temperature from 300 K to 393 K (see **Figure S3** of Supporting Information).

Figure 5 shows O...H interactions between SO_3^- group (of $[\text{TfO}^-]$ anions or Nafion) and acidic hydrogen of the ammonium cation. A sharp peak at 1.8 Å shows the presence of strong hydrogen bonding. This is also consistent with the N-S RDF peak at ~ 4 Å as seen in **Figure 3b** and **c**. The peak height of O-H RDF decreases with an increase of Nafion:PIL ratio. An increase in temperature from 300 K to 393 K results in decrease in the O...H interactions for respective Nafion:PIL ratio. These O...H interactions are not seen for acidic hydrogen (H_N) of cation and fluorine atoms of $[\text{TfO}^-]$ anion or Nafion. These structural correlations are further characterized by SDFs for these PIL doped Nafion composite.

3.2 Spatial Distribution Functions

A three dimensional spatial density map is calculated for the S-atom of SO_3^- group (of $[\text{TfO}^-]$ anion or Nafion) around the N-atom of ammonium cation. The calculated SDFs at 300 K for all Nafion:PIL ratios are shown in **Figure 6**. The density distribution of SO_3^- group around the center of mass of cation shows that the most preferred binding site of SO_3^- group is opposite to an acidic proton of $[\text{dema}^+]$. The density distribution of $[\text{TfO}^-]$ anions along the N-H bond vector is more dense over quaternary ammonium acidic proton. A comparison of spatial density maps for different Nafion:PIL ratios ($\text{C}_{1/1}$, $\text{C}_{1/2}$ and $\text{C}_{1/3}$) shows that the spatial density distribution of SO_3^- ions increases significantly at the acidic site of the ammonium cation. However, the calculated spatial density distribution of SO_3^- ions of Nafion is narrower than that of $[\text{TfO}^-]$. Further, the SO_3^- distribution is also seen around

the alkyl tails of the ammonium cation which is due to the existence of weak hydrogen bonding interactions between the alkyl hydrogen atoms of $[\text{dema}^+]$ and oxygen atoms of SO_3^- group.²⁷ This SO_3^- distribution along the alkyl tails becomes more diffused for $[\text{TfO}^-]$ anion with an increase in Nafion:PIL ratios. However, it remains unchanged for SO_3^- group of Nafion in $\text{C}_{1/1}$, $\text{C}_{1/2}$ and $\text{C}_{1/3}$. Thus, the interactions of SO_3^- group of Nafion with hydrogen atoms of alkyl tails of the ammonium cation are minimal.

3.3 Scattering Intensity

In order to characterize the nanostructure of PIL doped Nafion membrane, the partial structure factor is calculated from the Fourier transform of the $g(r)$ ^{42,43} (at 300 K and 393 K) for N-S atoms (see **Figure S4** of Supporting Information) and is written as

$$S_{ij}(q) = 4\pi\rho \int_0^\infty r^2 dr (g_{ij}(r) - 1) \frac{\sin qr_{ij}}{qr_{ij}} \quad (2)$$

where, ρ is the atomic density, q is momentum transfer for the scattering wavelength (λ_m), $g_{ij}(r)$ is the RDF from atom types i and j , r_{ij} is the inter-molecular distance between atom i and j , $S_{ij}(q)$ is the partial structure factor between atom types i and j . The scattering intensity ($I_{ij}(q)$) is calculated from partial structure factor such as⁴²

$$I_{ij}(q) = \sum_{ij} x_i x_j f_i(q) f_j(q) \frac{\sin qr_{ij}}{qr_{ij}} + \sum_{i \leq j} x_i x_j f_i(q) f_j(q) S_{ij}(q) \quad (3)$$

where, x_i and x_j are the atomic fraction of atoms i and j respectively, $f_i(q)$ and $f_j(q)$ are the q dependent atomic scattering factor for atoms i and j respectively.⁴² The peak profiles

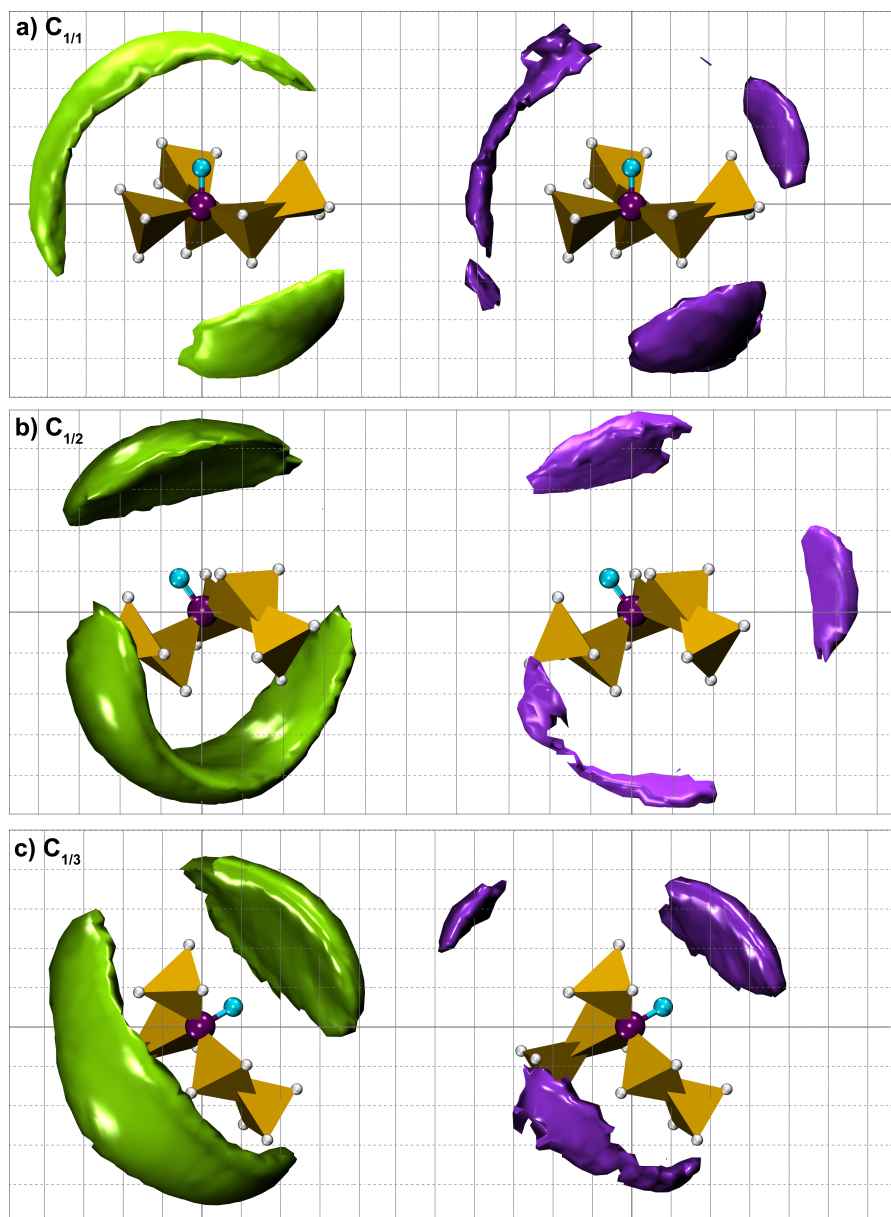


Fig. 6 Spatial density map of SO_3^- (S-atom) around the center of mass of ammonium cation (left: N- S_{TFO} and right: N- S_{Nafion}) calculated from MD simulations at 300 K for a) $C_{1/1}$, b) $C_{1/2}$, and c) $C_{1/3}$ respectively. [Colour scheme for (i) cation: N-purple (CPK), H_N -cyan (CPK), C_{methyl} -orange (Polyhedra), $\text{C}_{\text{ethyl/propyl}}$ -violet (Polyhedra), alkyl H-white (CPK); (ii) S-atom iso-surface: S_{TFO} -green, and S_{Nafion} -violet; (iii) iso-surface value is 0.006 \AA^{-3} for SO_3^- of $[\text{TfO}^-]$, and 0.005 \AA^{-3} for SO_3^- of Nafion respectively]

of scattering intensities calculated from simulations (see **Figure 7**) shows qualitative similarities with experiments. The peak intensity at 1.1 \AA^{-1} (a characteristic ionomer peak for Nafion)³² increases with an increase in Nafion:PIL ratio which suggests an enlargement in size of ionic clusters with PIL concentration. Whereas, the variation in scattering intensity peak at lower wave region ($\sim 0.1 \text{ \AA}^{-1}$) does not follow the trend

seen at 1.1 \AA^{-1} as a function of PIL concentration. This is due to the heterogeneous ionic distribution of PIL in Nafion membrane matrix as seen in **Figure 2**. The similarities seen in scattering intensity peak profiles for both N- S_{TFO} and N- S_{Nafion} atomic pairs suggest that interactions of the ammonium cation with SO_3^- group (of $[\text{TfO}^-]$ anion or Nafion) are quite competitive and equivalent. These similarities in peak height

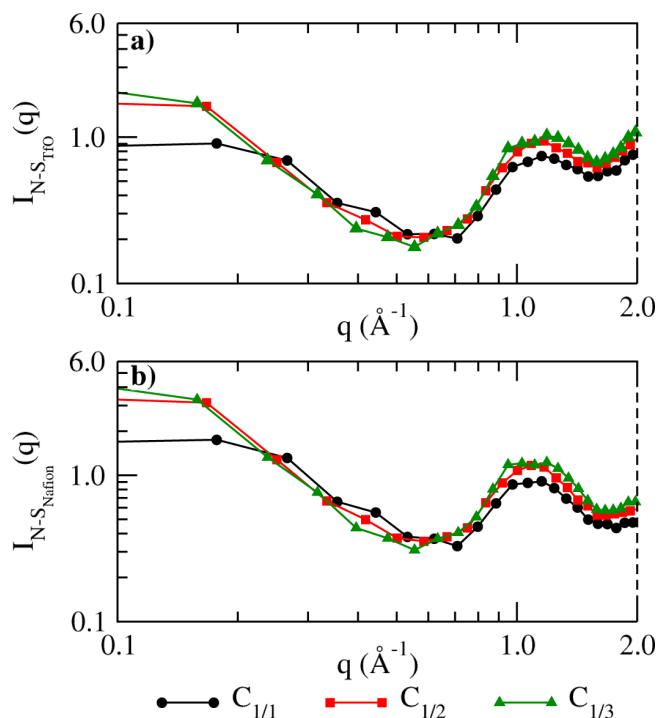


Fig. 7 Scattering intensities calculated at 300 K for a) N-S_{TfO}, and b) N-S_{Nafion} interactions respectively.

and peak positions point to the presence of localized ionic clusters of [dema⁺] and [TfO⁻] ions around the SO₃⁻ group of Nafion. This existence of localized ionic clusters agrees well with experimental observation on PIL doped composite membranes.^{16,19,21} The effect of temperature is insignificant on scattering intensity profiles as seen in **Figure S5** of Supporting Information.

3.4 Self-diffusion Coefficient and Nernst-Einstein Conductivity

Ionic mobility in anhydrous composite membrane is solely governed by PILs and can be examined by calculation of the Mean Square Displacement (MSD). The MSD as a function of time is calculated using the Einstein relationship⁴⁰ for [dema⁺] and [TfO⁻] ions. To extract the diffusive regime of ionic mobility, the exponent β is determined using Eqn. 4^{44,45} which can be written as

$$\beta(t) = \frac{d \ln(\text{MSD}(t))}{d \ln(t)} \quad (4)$$

The exponent $\beta(t) = 1$ represents diffusive behaviour of ions. The $\beta(t)$ plots as function of simulation time for cations and anions are shown in **Figure S6** of Supporting Information. For all Nafion:PIL ratios, the exponent $\beta(t)$ is found less than

one at 300 K which shows sub-diffusive behaviour of [dema⁺] and [TfO⁻] ions. At 393 K, this $\beta(t) \sim 1$. The self-diffusion coefficients (D^+ and D^- for [dema⁺] cations and [TfO⁻] ions respectively) are calculated from the diffusive regime (see **Figure S6** of Supporting Information) of MSD.

The calculated D^+ and D^- values are shown in **Table 2**. The self-diffusion coefficient of [dema⁺] and [TfO⁻] increases with an increase Nafion:PIL ratio. The influence of PIL concentration on ionic mobility of ions is more significant at high temperature (393 K). For example, the D^+ of [dema⁺] increases by a factor of 3.7 with an increase in Nafion:PIL ratio from C_{1/1} to C_{1/2} at 393 K. For all Nafion:PIL ratios, the diffusion of [dema⁺] and [TfO⁻] is 10-50 times larger at 393 K compared to 300 K. The calculated diffusivity of [dema⁺] is comparable with [TfO⁻] ions. Lee et al.¹² showed that ionic conductivity of [dema][TfO] doped polymer composite approaches to the bulk ionic liquid with increase in PIL doping under anhydrous condition. Recently, Sood et al.¹⁶ also observed that ionic conductivity of triethylamine triflate doped Nafion increases with increase in PIL content in membrane matrix. Using the diffusion coefficients of PIL, ionic conductivity (σ_{NE}) is determined using the Nernst-Einstein equation⁴³ and can be written as:

$$\sigma_{NE} = \frac{N_i q^2}{V k_B T} (D^+ + D^-) \quad (5)$$

where V is the volume, T is temperature, N_i is the total number of ion-pairs, q is the effective net charge on the ions, k_B is the Boltzmann constant, D^+ and D^- are self-diffusion coefficients of [dema⁺] cations and [TfO⁻] anions respectively. At higher PIL doping, the calculated σ_{NE} conductivity approaches to the conductivity of bulk [dema][TfO] PIL at 393 K (i.e. 4.3 S m⁻¹)²⁴. Thus, the trends seen in self-diffusion coefficients and σ_{NE} are qualitatively similar to the experiments.^{12,16}

4 Conclusions

An atomic-level understanding of interfacial characteristic of quasi-solid Nafion membrane comprising with [dema][TfO] PIL is presented using classical MD simulations. Interactions of the ammonium cation with the SO₃⁻ group of [TfO⁻] anion and Nafion membrane are similar. The intensity of hydrogen bond interactions between the ammonium cation with SO₃⁻ group decreases with an increase in Nafion:PIL ratios. This impact of increase in PIL doping is reflected in spatial density maps of SO₃⁻ distribution at the acidic site of the ammonium cation. The SO₃⁻ distribution over N-H bond vector becomes broad with increase in PIL concentration. The existence of weak hydrogen bonding between the alkyl tail length of the ammonium cation and [TfO⁻] anion is seen from SDFs and the distribution of SO₃⁻ group around the alkyl tails increases

Table 2 Self-diffusion coefficients and Nernst-Einstein conductivity (σ_{NE}) of ammonium-triflate ILs calculated from MD simulations.

System	Self-diffusion Coefficient ($\times 10^{-6} \text{ cm}^2 \text{ s}^{-1}$)				σ_{NE} (S m^{-1})	
	$D_{300\text{K}}^+$	$D_{300\text{K}}^-$	$D_{393\text{K}}^+$	$D_{393\text{K}}^-$	300 K	393 K
$\text{C}_{1/1}$	0.021	0.021	0.307	0.439	0.018	0.234
$\text{C}_{1/2}$	0.029	0.032	1.129	1.353	0.043	1.245
$\text{C}_{1/3}$	0.037	0.039	2.203	2.302	0.067	2.889

with Nafion:PIL ratios. Whereas, in case of SO_3^- group of Nafion, these weak hydrogen bonding interactions are moderate and least influenced by PIL doping. The temperature rise from 300 K to 393 K results in softening of the hydrogen bonding interactions between the acidic proton of the ammonium cation and oxygen atoms of SO_3^- group.

An ionomer peak obtained in calculated scattering intensity profiles clearly distinguish ion solvation around the SO_3^- groups and the existence of hydrophobic domains in composite membrane matrix. The self-diffusion coefficients and Nernst-Einstein conductivity calculated from MD simulations shows increase in ionic mobility with Nafion:PIL ratios and temperature. The trends in calculated diffusion of ions and ionic conductivities show qualitative agreement with experimental studies of Lee et al.¹² and Sood et al.¹⁶ on anhydrous PIL doped polymer composite. The influence of Coulomb forces and induced polarization on interionic structural ordering⁴⁶⁻⁴⁹ and interfacial structure of these composite membranes can be explored (using force-field refinement) and this can be the focus of future activities.

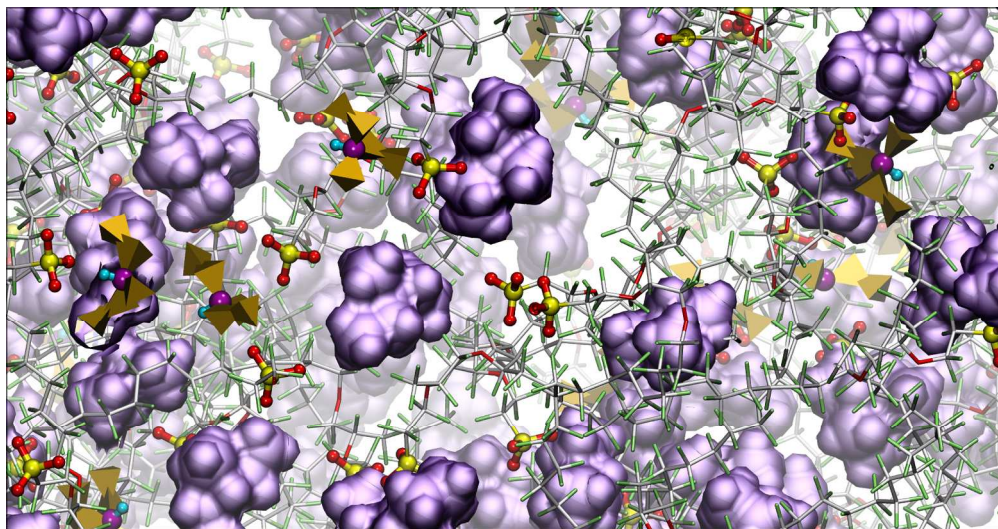
5 Acknowledgement

The author thanks Center for Development of Advanced Computing, Pune for providing high performance computing PARAM resources. The author acknowledges Department of Science and Technology for INSPIRE Faculty Award (DST/INSPIRE/04/2014/015731) and YSS/2015/000239 for financial support.

References

- C. A. Angell, N. Byrne and J.-P. Belieres, *Acc. Chem. Res.*, 2007, **40**, 1228–1236.
- D. R. MacFarlane, M. Forsyth, P. C. Howlett, J. M. Pringle, J. Sun, G. Anat, W. Neil and E. I. Izgorodina, *Acc. Chem. Res.*, 2007, **40**, 1165–1173.
- Y. Bai, Y. Cao, J. Zhang, M. Wang, R. Li, P. Wang, S. M. Zakeeruddin and M. Grätzel, *Nat. Mater.*, 2008, **7**, 626–630.
- M. Armand, F. Endres, D. R. MacFarlane, H. Ohno and B. Scrosati, *Nat. Mater.*, 2009, **8**, 621–628.
- D. R. MacFarlane, N. Tachikawa, M. Forsyth, J. M. Pringle, P. C. Howlett, G. D. Elliott, J. H. Davis, M. Watanabe, P. Simon and C. A. Angell, *Energy Environ. Sci.*, 2014, **7**, 232–250.
- M. V. Fedorov and A. A. Kornyshev, *Chem. Rev.*, 2014, **114**, 2978–3036.
- G. GebresilassieEshetu, M. Armand, B. Scrosati and S. Passerini, *Angew. Chem. Int. Ed.*, 2014, **53**, 13342–13359.
- M. Díaz, A. Ortiz and I. Ortiz, *J. Membr. Sci.*, 2014, **469**, 379–396.
- Y. Lu, K. Korf, Y. Kambe, Z. Tu and L. A. Archer, *Angew. Chem. Int. Ed.*, 2014, **53**, 488–492.
- I. Do and L. T. Drzal, *ACS Appl. Mater. Interfaces*, 2014, **6**, 12126–12136.
- J. Luo, A. H. Jensen, N. R. Brooks, J. Sniekers, M. Knipper, D. Aili, Q. Li, B. Vanroy, M. Wubbenhorst, F. Yan, L. Van Meervelt, Z. Shao, J. Fang, Z.-H. Luo, D. E. De Vos, K. Binnemans and J. Fransaer, *Energy Environ. Sci.*, 2015, DOI: 10.1039/c4ee02280g.
- S.-Y. Lee, A. Ogawa, M. Kanno, H. Nakamoto, T. Yasuda and M. Watanabe, *J. Am. Chem. Soc.*, 2010, **132**, 9764–9773.
- V. Di Noto, E. Negro, J.-Y. Sanchez and C. Iojoiu, *J. Am. Chem. Soc.*, 2010, **132**, 2183–2195.
- V. Di Noto, M. Piga, G. A. Giffin, S. Lavina, E. S. Smotkin, J.-Y. Sanchez and C. Iojoiu, *J. Phys. Chem. C*, 2011, **116**, 1361–1369.
- V. Di Noto, M. Piga, G. A. Giffin, S. Lavina, E. S. Smotkin, J.-Y. Sanchez and C. Iojoiu, *J. Phys. Chem. C*, 2011, **116**, 1370–1379.
- R. Sood, C. Iojoiu, E. Espuche, F. Gouanv, G. Gebel, H. Mendil-Jakani, S. Lyonnard and J. Jestin, *J. Phys. Chem. C*, 2012, **116**, 24413–24423.
- T. Yasuda, S.-i. Nakamura, Y. Honda, K. Kinugawa, S.-Y. Lee and M. Watanabe, *ACS Appl. Mater. Interfaces*, 2012, **4**, 1783–1790.
- D. Langevin, Q. T. Nguyen, S. Marais, S. Karademir, J.-Y. Sanchez, C. Iojoiu, M. Martinez, R. Mercier, P. Judeinstein and C. Chappéy, *J. Phys. Chem. C*, 2013, **117**, 15552–15561.
- F. Lu, X. Gao, X. Yan, H. Gao, L. Shi, H. Jia and L. Zheng, *ACS Appl. Mater. Interfaces*, 2013, **5**, 7626–7632.
- F. Lu, X. Gao, S. Xie, N. Sun and L. Zheng, *Soft Matter*, 2014, **10**, 7819–7825.
- R. Sood, C. Iojoiu, E. Espuche, F. Gouanv, G. Gebel, H. Mendil-Jakani, S. Lyonnard and J. Jestin, *J. Phys. Chem. C*, 2014, **118**, 14157–14168.
- S. Liu, L. Zhou, P. Wang, F. Zhang, S. Yu, Z. Shao and B. Yi, *ACS Appl. Mater. Interfaces*, 2014, **6**, 3195–3200.
- T. Yasuda and M. Watanabe, *Supported Protic Ionic Liquids in Polymer Membranes for Electrolytes of Nonhumidified Fuel Cells*, Wiley-VCH Verlag GmbH & Co. KGaA, 2014, pp. 407–418.
- H. Nakamoto and M. Watanabe, *Chem. Commun.*, 2007, 2539–2541.
- L. Johnson, A. Ejigu, P. Licence and D. A. Walsh, *J. Phys. Chem. C*, 2012, **116**, 18048–18056.
- A. P. Sunda, V. M. Dhavale, S. Kurungot and A. Venkatnathan, *J. Phys. Chem. B*, 2014, **118**, 1831–1838.
- A. P. Sunda, A. Mondal and S. Balasubramanian, *Phys. Chem. Chem. Phys.*, 2015, **17**, 4625–4633.
- A. Ejigu and D. A. Walsh, *J. Phys. Chem. C*, 2014, **118**, 7414–7422.
- J. W. Blanchard, J.-P. Belières, T. M. Alam, J. L. Yarger and G. P. Holland,

- J. Phys. Chem. Lett.*, 2011, **2**, 1077–1081.
- 30 B. Hess, C. Kutzner, D. van der Spoel and E. Lindahl, *J. Chem. Theor. Comput.*, 2008, **4**, 435–447.
- 31 A. P. Sunda and A. Venkatnathan, *Soft Matter*, 2012, **8**, 10827–10836.
- 32 A. P. Sunda and A. Venkatnathan, *J. Mater. Chem. A*, 2013, **1**, 557–569.
- 33 T. M. Chang, L. X. Dang, R. Devanathan and M. Dupuis, *J. Phys. Chem. A*, 2010, **114**, 12764–12774.
- 34 L. Martínez, R. Andrade, E. G. Birgin and J. M. Martínez, *J. Comput. Chem.*, 2009, **30**, 2157–2164.
- 35 T. Darden, D. York and L. Pedersen, *J. Chem. Phys.*, 1993, **98**, 10089–10092.
- 36 U. Essmann, L. Perera, M. L. Berkowitz, T. Darden, H. Lee and L. G. Pedersen, *J. Chem. Phys.*, 1995, **103**, 8577–8593.
- 37 G. Bussi, D. Donadio and M. Parrinello, *J. Chem. Phys.*, 2007, **126**, 014101.
- 38 H. J. C. Berendsen, J. P. M. Postma, W. F. van Gunsteren, A. DiNola and J. R. Haak, *J. Chem. Phys.*, 1984, **81**, 3684–3690.
- 39 W. Humphrey, A. Dalke and K. Schulten, *J. Mol. Graphics*, 1996, **14**, 33–38.
- 40 M. P. Allen and D. J. Tildesley, *Computer Simulation of Liquids*, Clarendon Press, New York, NY, USA, 1989.
- 41 R. Devanathan, A. Venkatnathan and M. Dupuis, *J. Phys. Chem. B*, 2007, **111**, 8069–8079.
- 42 T. Head-Gordon and G. Hura, *Chem. Rev.*, 2002, **102**, 2651–2670.
- 43 J.-P. Hansen and I. R. McDonald, *Theory of Simple Liquids, Third Edition*, Academic Press, 3rd edn., 2006.
- 44 E. J. Maginn, *Acc. Chem. Res.*, 2007, **40**, 1200–1207.
- 45 M. G. Del Pópolo and G. A. Voth, *J. Phys. Chem. B*, 2004, **108**, 1744–1752.
- 46 T.-M. Chang and L. X. Dang, *J. Phys. Chem. A*, 2009, **113**, 2127–2135.
- 47 T. Yan, Y. Wang and C. Knox, *J. Phys. Chem. B*, 2010, **114**, 6905–6921.
- 48 M. Kohagen, M. Brehm, J. Thar, W. Zhao, F. Müller-Plathe and B. Kirchner, *J. Phys. Chem. B*, 2011, **115**, 693–702.
- 49 C. Schroder, *Phys. Chem. Chem. Phys.*, 2012, **14**, 3089–3102.



Interfacial structure correlation of cation interactions with sulfonate groups (of anion or Nafion) in [dema][TfO] doped Nafion composite are competitive and equivalent.